

# OptGM: An Optimized Gate Merging Method to Mitigate NBTI in Digital Circuits

Maryam Ghane, Amir M. Hajisadeghi, Hamid R. Zarandi\*

Department of Computer Engineering, Amirkabir University of Technology (Tehran Polytechnic)

**Abstract:** This paper presents OptGM, an optimized gate merging method designed to mitigate negative bias temperature instability (NBTI) in digital circuits. First, the proposed approach effectively identifies NBTI-critical internal nodes—those with a signal probability exceeding a predefined threshold. Next, based on the proposed optimized algorithm, the sensitizer gate—which drives the critical node—and the sensitive gate, which is fed by it, are merged into a new complex gate. This complex gate preserves the original logic while eliminating NBTI-critical nodes. Finally, to evaluate the effectiveness of OptGM, we assess it on several combinational and sequential benchmark circuits. Simulation results demonstrate that, on average, the number of NBTI-critical transistors (i.e., PMOS transistors connected to critical nodes), NBTI-induced delay degradation, and the total transistor count are reduced by 89.29%, 23.87%, and 6.47%, respectively. Furthermore, OptGM enhances performance per cost (PPC) by 12.8% on average, with minimal area overhead.

**Index Terms**— Digital Circuit, Gate Merging, Negative Bias Temperature Instability (NBTI), Signal Probability.

## 1- Introduction

With continued technology scaling and thinner gate oxide layers, circuit aging has become a significant reliability challenge, particularly in nanometer-scale designs [1]. Negative bias temperature instability (NBTI) [2-4], positive bias temperature instability (PBTI) [5], hot carrier injection (HCI) [6, 7], and time-dependent dielectric breakdown (TDDDB) [8] are the primary factors contributing to circuit aging and performance degradation. Among these, NBTI has gained increased attention as a critical reliability concern due to the aggressive downscaling of semiconductor technology nodes, which results in thinner gate oxides in highly scaled designs [1, 9].

NBTI affects PMOS transistors when they are negatively biased, leading to degradation in electrical parameters such as increased threshold voltage, reduced transconductance, decreased linear and saturation current, lower channel mobility, and increased subthreshold swing [10]. Over time, these effects manifest as delay faults, potentially leading to system failure. NBTI follows a two-phase process: stress and recovery [1, 10]. During the stress phase, NBTI occurs when PMOS transistors are ON ( $|V_{gs}| > |V_{th}|$ ), causing a significant increase in the absolute threshold voltage over time. Conversely, in the recovery phase, when PMOS transistors are OFF ( $|V_{gs}| < |V_{th}|$ ), part of the degraded threshold voltage is recovered [1].

Several methods have been proposed to enhance the NBTI tolerance of digital circuits. Input vector control (IVC) methods manipulate input vectors to alter the zero probability of internal PMOS transistors [11-13]. However, their effectiveness is limited because internal nodes at deeper circuit levels are less controllable through input vectors. On the other hand, internal node control (INC) methods offer better controllability of internal nodes for NBTI mitigation [14-18]. The gate replacement method, a form of INC, replaces gates connected to NBTI-critical nodes to mitigate NBTI effects [17]. However, mostly due to the high design overhead, it can only be applied to a limited number of critical internal nodes. Another INC approach leverages sleep signals to control critical internal nodes by introducing transmission gates [15]. This method uses both PMOS and NMOS transistors, but the additional PMOS transistors remain susceptible to NBTI aging, leading to considerable delay, power, and area overheads.

Based on the above explanations, there is a clear need for an effective, low-overhead method to mitigate NBTI in digital circuits. Since NBTI-induced degradation strongly depends on the stress time of PMOS transistors, this paper presents a method that removes NBTI stress from transistors with long stress time. The proposed method first identifies NBTI-critical internal nodes by calculating their zero signal probability ( $SP_0$ ). A node is classified as critical if its  $SP_0$  exceeds a predefined threshold. Next, NBTI-critical nodes are removed by merging NBTI-sensitive gates and NBTI-sensitizer gates. The sensitive gate is driven by the critical node, while the sensitizer gate determines its value. Through this gate merging process, a new complex gate is formed with the same logic function, effectively eliminating NBTI-critical nodes.

\* Corresponding author.

E-mail address: h\_zarandi@aut.ac.ir (Hamid R. Zarandi)

The choice of  $SP_0$  threshold significantly influences circuit performance and area overhead. A lower threshold classifies more nodes as critical, leading to increased circuit lifetime but also higher area overhead due to additional complex gates. Conversely, a higher threshold results in fewer critical nodes, offering minimal NBTI improvement. To balance performance and area overhead, this work introduces a performance per cost (PPC) metric, which optimizes the trade-off between circuit performance (delay) and area consumption. The method evaluates  $SP_0$  threshold values from  $\{0.5, 0.65, 0.75, 0.85, 0.95\}$ , selecting the one that maximizes PPC. Using this optimization, the average PPC across circuits improves by 12.8% compared to a fixed threshold value of 0.5.

The proposed method was evaluated on a subset of combinational and sequential circuits from the ISCAS'85 and ISCAS'89 benchmark suites. Results show that it reduces NBTI-critical transistors (i.e., PMOS transistors connected to critical nodes) by 89.29%, lowers the total transistor count by 6.47% on average, and mitigates NBTI-induced delay degradation by 23.87% over 10 years of operation. Despite these improvements, it incurs only a 1.8% area overhead, demonstrating its efficiency and practicality for NBTI mitigation. The key contributions of this paper are as follows:

- Proposing OptGM, an optimized gate merging method for NBTI mitigation in digital circuits.
- Introducing the PPC metric to select the optimal  $SP_0$  threshold by balancing NBTI mitigation with delay and area overhead.
- Designing an algorithmic framework that identifies NBTI-critical internal nodes and merges sensitizer and sensitive gates into complex gates.
- Conducting a comprehensive evaluation that demonstrates the high efficiency of the method in reducing NBTI degradation with negligible area overhead.

The remainder of this paper is structured as follows. Section 2 provides background on NBTI phenomena and NBTI models. Section 3 reviews related work. Section 4 describes the proposed NBTI mitigation method in detail. Section 5 presents evaluation results on benchmark circuits. Finally, Section 6 concludes the paper.

## 2- Background

NBTI causes degradation in the key electrical parameters of stressed devices, such as threshold voltage, transconductance, linear and saturation current, channel mobility, and subthreshold swing [10]. This section first describes the NBTI phenomenon and then discusses the main factors that intensify it.

### 2-1- NBTI Phenomenon

A widely used model to explain NBTI is the Reaction-Diffusion (R-D) model [10, 19, 20], which highlights the central role of hole-trapping mechanisms in NBTI behavior. According to this model, NBTI occurs when a PMOS transistor is turned ON ( $|V_{gs}| > |V_{th}|$ ) and a vertical electric field is present across the gate oxide. During the stress phase, when a negative bias is applied to the gate of a PMOS transistor, relatively weak Si-H bonds at the silicon-oxide interface are broken due to the electric field. This causes hydrogen atoms to diffuse into the dielectric, forming positive interface traps and molecular hydrogen [10, 19]. The positive charge accumulation shifts the threshold voltage in the positive direction, which contributes to circuit aging. As a result, the absolute value of the threshold voltage increases significantly over time [1, 10].

A particular characteristic of NBTI is its partial recoverability. In the recovery phase, when the PMOS transistor is OFF ( $|V_{gs}| < |V_{th}|$ ), hydrogen diffuses back toward the interface and anneals the broken silicon bonds, allowing some of the Si-H bonds to be reformed. This reduces the number of interface traps and leads to partial recovery of the threshold voltage [10, 19].

Fig. 1 illustrates four major factors that influence NBTI: 1) stress time, 2) signal probability, 3) temperature, and 4) vertical electric field. Fig. 1(a) shows the threshold voltage variation over time during the stress and recovery phases for 90nm PMOS transistors [1, 10, 19]. In the stress phase, the threshold voltage increases, aging the PMOS transistors and degrading circuit performance. In the recovery phase, the threshold voltage partially recovers [1, 10, 19]. Stress time affects threshold voltage with time radically ( $\Delta V_{th} \propto t^n$ ,  $n \approx 0.25$ ). Moreover, zero signal probability ( $SP_0$ ) increases the absolute value of threshold voltage dramatically ( $\Delta V_{th} \propto (SP_0)^n$ ). Temperature (Fig. 1(b)) and vertical electric field (Fig. 1(c)) also have an impact on NBTI. These parameters increase the absolute value of threshold voltage exponentially ( $\Delta V_{th} \propto e^T$ ,  $\Delta V_{th} \propto e^{E_{ox}}$ ) [1, 10, 19].

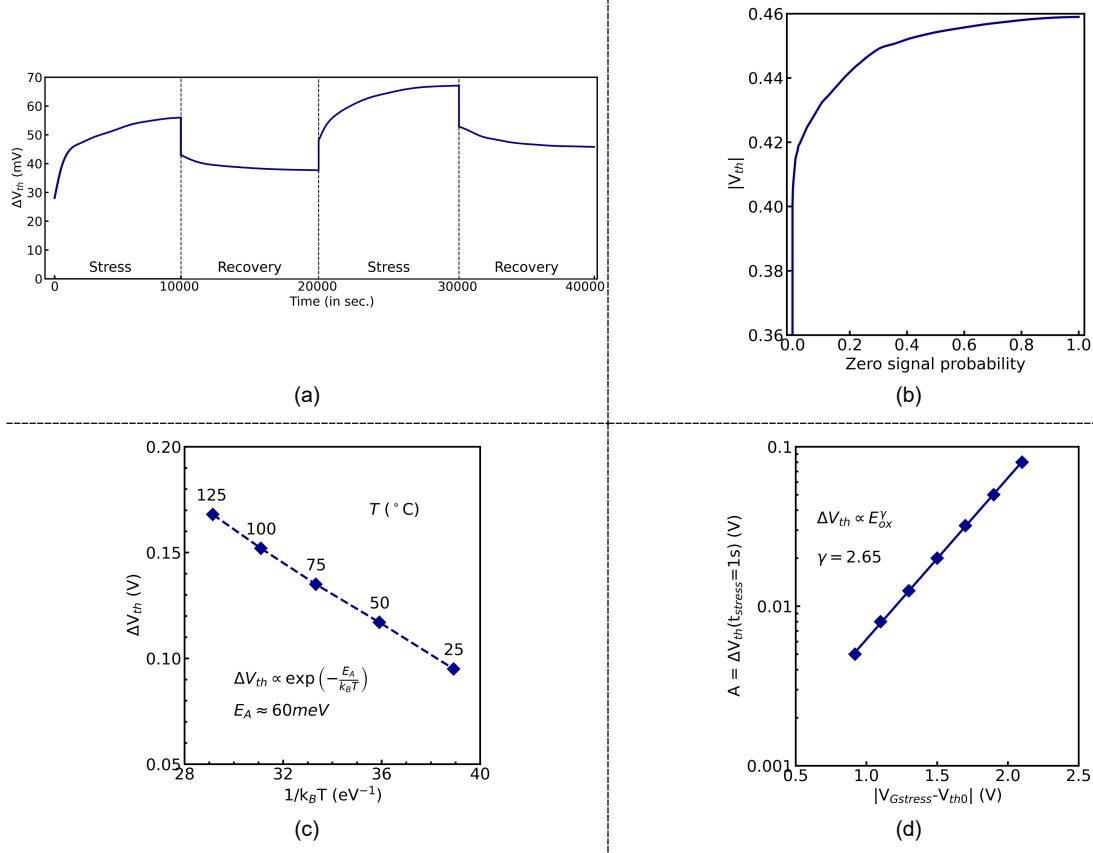


Fig. 1. Four major factors in the occurrence of NBTI: a) stress time, b) zero signal probability c) temperature, and d) vertical electric field.

## 2-1- NBTI Model

The variation in threshold voltage ( $\Delta V_{th}$ ) during the stress and recovery phases can be modeled by the following equations [1]:

$$\Delta V_{th}(t) = \left( K_v (t-t_0)^{0.5} + \sqrt{\Delta V_{th}(t_0)} \right)^{2n} \quad (1)$$

$$\Delta V_{th}(t) = \Delta V_{th}(t_1) \left( 1 - \frac{2\varepsilon_1 \cdot t_e + \sqrt{\varepsilon_2 \cdot C \cdot (t-t_1)}}{(1+\delta) \cdot t_{ox} + \sqrt{C \cdot t}} \right) \quad (2)$$

Here,  $t_0$  and  $t_1$  denote the start times of the stress and recovery phases, respectively, and  $t$  is the elapsed stress time.  $K_v$  depends on temperature and electric field;  $\varepsilon_1$ ,  $\varepsilon_2$ , and  $C$  are temperature-dependent constants;  $t_{ox}$  and  $t_e$  denote the oxide thickness and effective oxide thickness, respectively;  $\delta$  is a fitting parameter less than 1.

A closed-form expression for the overall  $\Delta V_{th}$  after accounting for both stress and recovery phases can be given as [1]:

$$\Delta V_{th}(t) = \left( \frac{\sqrt{K_v^2 \cdot \alpha \cdot T_{clk}}}{1 - \beta_t^{2n}} \right)^{2n} \quad (3)$$

$$\beta_t = 1 - \frac{2\varepsilon_1 \cdot t_e + \sqrt{\varepsilon_2 \cdot C \cdot (1-\alpha) \cdot T_{clk}}}{2t_{ox} + \sqrt{C \cdot t}} \quad (4)$$

where  $\alpha$  denotes the stress probability,  $T_{clk}$  is the clock period, and  $n$  typically varies between 0.1 and 0.25, depending on the technology. Thus, stress probability ( $\alpha$ ) plays a critical role in determining the severity of NBTI and is a key parameter in designing NBTI mitigation strategies for digital circuits [2, 19].

### 3- Related Work

Several methods have been proposed to enhance the tolerance of digital circuits against NBTI. As shown in Fig. 2, these methods are generally categorized into two main groups: 1) compensation methods, and 2) mitigation methods. Compensation methods typically utilize techniques such as transistor/gate sizing [21, 22] threshold voltage ( $V_{th}$ ) tuning [20, 23], and guard banding [24, 25] to counteract the destructive effects of NBTI. These approaches aim to extend circuit lifetime by minimizing the impact of NBTI on device parameters. On the other hand, mitigation methods can be further divided into design-time methods and adaptive methods. Design-time techniques include NBTI-aware logic synthesis [20, 26, 27], input vector control (IVC) [11-13], and internal node control (INC) methods [14-18].

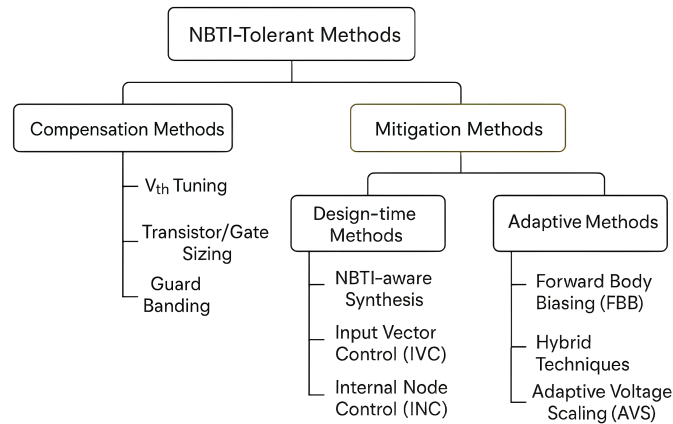


Fig. 2. Classification of NBTI-tolerant methods.

The method proposed in [28] introduces an NBTI-aware digital low-dropout regulator with adaptive gain scaling control, achieving a 33% improvement in mitigating NBTI effects. Several IVC-based approaches [11-13] aim to reduce NBTI degradation by adjusting input vectors and performing transistor reordering. These methods modify the zero signal probability of internal nodes to reduce stress on PMOS transistors. However, their effectiveness is limited in large circuits because internal nodes at deeper levels are less controllable via external input vectors, and consequently, NBTI mitigation applies to only a small subset of transistors.

INC-based approaches address this limitation by directly controlling internal nodes to suppress NBTI effects. Some INC methods achieve this by inserting sleep transistors into gates or internal paths [15, 29]. For instance, the method in [15, 29] proposes adding a sleep signal that controls internal nodes during standby mode. Bild et al. [29] assume that the system can generate sleep signals to load new external inputs and activate pre-selected internal signals for internal node control. This method modifies pull-up and pull-down networks by inserting NMOS and PMOS transistors. Although it reduces NBTI, it also increases leakage power and necessitates structural changes to all gates in the library, requiring custom gate redesign and replacement.

Wang et al. [17] propose a gate replacement technique using existing library gates to insert a sleep signal. However, this method can only be applied to a limited number of NBTI-critical internal nodes due to library constraints. Moreover, it does not account for timing overheads introduced by the gate replacement, which may adversely affect the critical path delay. Another INC-based method [15] proposes controlling internal nodes by inserting sleep signals using two PMOS and one NMOS transistor. While this reduces NBTI, the added PMOS transistors are themselves prone to NBTI-induced degradation, and the method imposes substantial delay and power overhead.

The method presented in [30] uses an adaptive body biasing technique and achieves significant NBTI reduction, decreasing total yield loss by 97.1% after 10 years. However, it increases both dynamic power and leakage power during the first five years. Other adaptive methods [31, 32] use forward body biasing (FBB) to reduce threshold voltage and improve performance. However, this exponentially increases subthreshold leakage. Dynamic voltage and frequency scaling (DVFS) techniques [33] are also utilized to manage threshold voltage dynamically. Consequently, hybrid techniques that combine FBB and adaptive voltage scaling [34] have been proposed to achieve better trade-offs between power consumption and NBTI mitigation.

In this paper, under the INC category, we propose a gate-merging approach that aims to be more effective and efficient than the existing INC methods, which often incur high overhead. Method [14] previously introduced a

gate-merging technique to mitigate NBTI in digital circuits. While that approach effectively reduces NBTI, it relies on a static and unoptimized selection of NBTI-critical internal nodes for merging. In contrast, the present study introduces a performance-per-cost metric and novel algorithms for the systematic selection of NBTI-critical nodes and gate merging. This enables effective NBTI mitigation with minimal overhead. The proposed method ensures that, for each circuit, a good trade-off between NBTI reduction and overhead (in terms of area and performance) is achieved.

## 4- The Proposed Method: Optimized Gate Merging

This section introduces OptGM, an optimized gate merging method to mitigate NBTI-induced degradation in digital circuits by eliminating NBTI-critical internal nodes. The proposed method comprises two main phases. First, it identifies NBTI-critical PMOS transistors—those with high-stress probability—by estimating the zero signal probability ( $SP_0$ ) of internal nodes. A transistor is considered critical if it remains ON for a significant portion of time, which corresponds to an internal node with an  $SP_0$  above a predefined threshold.

Once the NBTI-critical internal nodes are identified, OptGM removes them by merging their driving and driven gates into a new complex gate that implements the equivalent logic. This process eliminates the critical node and its associated PMOS transistor, thereby reducing NBTI-induced degradation.

The threshold for determining criticality is circuit-specific and selected using the performance per cost (PPC) metric, which balances delay reduction against area overhead. A higher threshold removes more transistors but increases complexity; a lower one reduces overhead but limits NBTI improvement.

### 4-1- Fundamental Concepts and Definitions

Before detailing the proposed optimized gate merging algorithm, the key terms and assumptions are defined.

**Signal Probability:** The probability that a node holds logic '0' or '1', denoted as  $SP_0$  and  $SP_1$ , respectively. For a node  $n$ ,  $SP_0(n) = 1 - SP_1(n)$ .  $SP_0$  is used to estimate the stress probability of PMOS transistors connected to internal nodes. A higher  $SP_0$  indicates the transistor is ON longer, contributing more to NBTI.  $SP_0$  values for internal nodes are derived from the signal probabilities of primary logic gates, as shown in Table 1.

Table 1.  $SP_1$  calculation of primary gates

Primary gate	Inputs $SP_1$	Output $SP_1$ calculation
NOT	$S_1$	$1-S_1$
AND	$S_1, S_2$	$S_1 \times S_2$
OR	$S_1, S_2$	$S_1+S_2-(S_1 \times S_2)$

**NBTI-Critical Node:** An internal node is considered NBTI-critical if its  $SP_0$  exceeds a predefined threshold. This threshold reflects the acceptable upper limit of transistor stress in the circuit. Critical nodes are targeted for elimination through gate merging.

**Threshold Value:** A tunable parameter that defines the  $SP_0$  boundary for node criticality. Lower values mark more nodes as critical—enhancing mitigation but potentially increasing area. The optimal threshold is selected using:

$$\text{Performance Per Cost (PPC)} = \frac{1}{\text{Delay}} = \frac{1}{\text{Delay} \times \text{Area}} \quad (5).$$

In this paper, NBTI-induced degradation is calculated for different threshold values. The threshold value that the PPC of the modified circuit has a maximum value, is considered as the best threshold value for that circuit. It should be noted that in many high-performance digital systems—such as datapath components in processors, real-time control logic in aerospace and industrial applications, and hardware accelerators for signal processing—delay and silicon area are the primary design constraints. While delay directly impacts system responsiveness and throughput, minimizing area reduces cost, enables higher integration, and satisfies form-factor constraints in embedded and mission-critical systems. Accordingly, the proposed PPC metric emphasizes these factors to align with practical design priorities in such NBTI-aware scenarios.

**Sensitive Gate:** A gate is sensitive if one of its inputs is an NBTI-critical internal node. For instance, in Fig. 3(a), the  $SP_0$  of node  $N_5$  is 0.75 and if the threshold is set to 0.75, then  $N_5$  is a NBTI-critical node. Therefore, gate  $G_3$  is a sensitive gate.

**Sensitizer Gate:** A gate is a sensitizer if its output is an NBTI-critical node, meaning it directly drives a high- $SP_0$  node and hence contributes to the stress of the connected PMOS transistor. For example, in Fig. 3(a), gate  $G_1$  is the sensitizer of node  $N_5$ .

**Complex Gate:** A gate formed by merging sensitizer and sensitive gates. It preserves the logic function and eliminates the internal node. Fig. 3(b) illustrates a complex gate generated by merging AND and NAND gates.

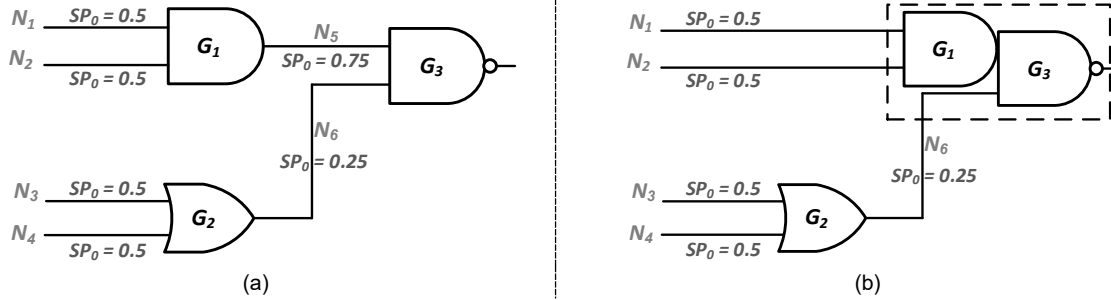


Fig. 3. An illustration of a) NBTI-critical node, sensitive and sensitizer gates and, b) merging of AND and NAND gates to generate a complex gate with logic function  $F = ((N_1 \cdot N_2) \cdot (N_3 + N_4))'$ .

#### 4-2- Optimal Gate Merging Algorithm

In order to reduce the NBTI-induced degradation, an optimal gate merging algorithm is proposed. It follows three main steps for each circuit: 1) NBTI criticality analysis, 2) gate merging, and 3) optimal threshold determination. Algorithm 1 coordinates these steps by invoking the *NBTI\_Criticality\_Analysis* (Algorithm 2) and *Gate\_Merging* (Algorithm 3) functions for each candidate threshold in a predefined set. Then, the threshold value that maximizes the PPC is selected as the optimal threshold value and used for the final application.

---

##### Algorithm 1: Optimal Gate Merging

---

**Input:** Netlist of the circuit

**Output:** Optimized NBTI-tolerant circuit

- 1 Threshold Set = {0.5, 0.65, 0.75, 0.85, 0.95};
  - 2 OGM\_Circuit\_Set = {};
  - 3 **foreach** T in Threshold Set **do**
  - 4     (NBTI\_Critical\_Nodes, Sensitizer\_Gates, Sensitive\_Gates) = *NBTI\_Criticality\_Analysis*(Circuit, T);
  - 5     GM\_Circuit = **Gate\_Merging** (Circuit, NBTI\_Critical\_Nodes, Sensitizer\_Gates, Sensitive\_Gates);
  - 6     GM\_PPC = Calculate PPC for GM\_Circuit;
  - 7     Insert (GM\_Circuit, GM\_PPC) to OGM\_Circuit\_Set;
  - 8 **end foreach**
  - 9 OGM\_Circuit = Circuit with maximum PPC from OGM\_Circuit\_Set;
  - 10 **return** (OGM\_Circuit);
- 

Algorithm 2 describes the NBTI criticality analysis step. It begins with leveling the circuit gates based on topological order. The  $SP_0$  of primary inputs is assumed to be 0.5 (though it may vary based on real input activity).  $SP_0$  values of all internal nodes are computed recursively using the gate-level structure and Table 1. Nodes exceeding the threshold are marked as NBTI-critical, and their sensitizer and sensitive gates are recorded.

Algorithm 3 describes the gate merging step. First, the NBTI-critical internal nodes of the circuit are identified separately for the critical path and the non-critical paths. Then, within each group, the nodes are sorted in descending order based on their  $SP_0$  values. This prioritization ensures that the nodes with the highest stress probability are handled first. Subsequently, the algorithm iterates over the sorted lists, giving priority to the critical path nodes, followed by the non-critical path nodes. For each selected NBTI-critical node, if both the associated sensitive and sensitizer gates are not already complex, they are merged into a new complex gate that preserves the original logic functionality. This merging process involves generating the Boolean expressions of the gates and combining them according to the complex gate generation rules [35, 36]. It should be noted that if a sensitizer gate has  $n$  fan-outs,  $n-1$  additional copies are created for merging. Also, merging is prioritized on the critical path to maximize delay benefits.

---

**Algorithm 2: NBTI Criticality Analysis of Circuit (*NBTI\_Criticality\_Analysis*)**

---

**Input:** Netlist of the circuit  $G = [g_1, g_2, \dots, g_n]$ , and threshold value ( $T$ )

**Output:** NBTI-critical nodes, sensitizers, and sensitive gates

```
1   $G_{sorted} = \text{topological\_order\_sort}(G)$ ;  
2   $L = \text{depth of netlist}$ ;  
3   $N = [n_1, n_2, \dots, n_m]$ ; // Internal nodes of circuit.  
  
4  // Calculate  $SP_0$  of internal nodes of circuit.  
5   $SP_0(\text{primary inputs}) = 0.5$ ;  
6  for  $i=1$  to  $L$  do  
7      foreach  $g$  in  $G_{sorted}(i)$  do  
8          | Calculate  $SP_0$  of the output node of the gate  $g$ ;  
9      end foreach  
10 end for  
  
11 // Determining NBTI-critical nodes.  
12 foreach  $n$  in  $N$  do  
13     | if  $SP_0(n) \geq T$  then  
14         | Node  $n$  is the NBTI-critical node;  
15     end if  
16 end foreach  
  
17 // Determining sensitive and sensitizer gates.  
18 foreach  $g$  in  $G$  do  
19     | if Output( $g$ ) is NBTI-critical node then  
20         | Gate  $g$  is sensitizer gate;  
21     end if  
22     | if Output( $g$ ) is NBTI-critical node then  
23         | Gate  $g$  is sensitive gate;  
24     end if  
25 end foreach  
26 return (NBTI_Critical_Nodes, Sensitizer_Gates, Sensitive_Gates);
```

---

---

**Algorithm 3: Merging Sensitizer and Sensitive Gates (*Gate\_Merging*)**

---

**Input:** Netlist of the circuit, NBTI-critical nodes, sensitizer, and sensitive gates

**Output:** NBTI-tolerant circuit

```
1   $F = [f_1, f_2, \dots, f_N]$ ; // Number of fan-out branches of node  $n$ .  
2   $Critical\_Path = \text{Find critical path of circuit}$ ;  
3   $Sorted\_NBTI\_critical\_nodes\_CP = \text{Sort NBTI-critical nodes in critical path of circuit in descent order based on } SP_0 \text{ value}$ ;  
4   $Non\_Critical\_Path = \text{Find non-critical paths of circuit}$ ;  
5   $Sorted\_NBTI\_critical\_nodes\_NonCP = \text{Sort NBTI-critical nodes in critical path of circuit in descent order based on } SP_0 \text{ value}$ ;  
  
6  foreach  $S$  in [ $Sorted\_NBTI\_critical\_nodes\_CP$ ,  $Sorted\_NBTI\_critical\_nodes\_NonCP$ ] do  
7      foreach  $n$  in  $S$  do  
8          | if sensitizer AND sensitive gates of node  $n$  are not complex gates then  
9              | if  $F(n) > 1$  then  
10                 | Create  $F(n)-1$  copy of sensitizer gate of node  $n$ ;  
11             end if  
12         end if  
13         | Convert into one complex gate (sensitizer gate of node  $n$ , sensitive gate of node  $n$ );  
14     end foreach  
15 end foreach  
16 return (GM_Circuit); // Gates merged circuit.
```

---

The overall timing complexity of Algorithm 1 is dominated by the sorting procedure in *Gate\_Merging* function (Algorithm 3), which is  $O(N \times \log N)$ , where  $N$  is the number of NBTI-critical nodes in the netlist. However, because the proposed optimal gate merging algorithm is executed during the implementation phase for each circuit, its time complexity would not be challenging.

It is worth mentioning that the effectiveness of the current version of the proposed method depends on the number of primary gates constituting the circuits under consideration. If a circuit is synthesized to the netlist with a high number of complex gates, not primary gates, although the proposed method can reduce the NBTI-induced degradation, merging the complex gates with high fanout gates will incur high area overhead due to not being optimized while compared to the gates in the library technology file. Nevertheless, in such cases, the proposed method can be effectively applied at the transistor level by designing NBTI-aware complex standard cells with OptGM incorporated at the transistor level.

Regarding the integration of the proposed method with ASIC design flow, this method can be incorporated with synthesis algorithms as an NBTI-aware synthesis process to reach a synthesized circuit with high robustness against NBTI phenomena. Alternatively, it can be applied after the synthesis process and before the placement process of design flow.

In the remainder of this section, two illustrative examples are provided to further clarify the proposed gate merging method. In the first example, Fig. 4(a) shows a 3-input transistor-level NOR circuit that implements the logic function  $((A + B)' + (C + D)')'$ . Assuming the  $SP_0$  of all inputs is 0.5, the resulting  $SP_0$  values of nodes  $m$  and  $n$  are each 0.75. This means that, statistically, the PMOS transistors connected to nodes  $m$  and  $n$  are ON 75% of the time. If the  $SP_0$  threshold is set to 0.75, nodes  $m$  and  $n$  are classified as NBTI-critical internal nodes. Consequently, gates  $G_1$  and  $G_2$  are identified as sensitizer gates, and  $G_3$  is the corresponding sensitive gate.

According to NOR logic, the Boolean expressions for  $G_1$  and  $G_2$  are  $G_1 = (A + B)'$  and  $G_2 = (C + D)'$ , respectively. The output of  $G_3$ , therefore, evaluates the expression  $(G_1 + G_2)'$  which simplifies to  $((A + B)' + (C + D)')'$ . Based on the complex gate generation rules [35, 36], this logic expression is converted into a single complex gate. By merging the sensitizer and sensitive gates, the internal NBTI-critical nodes ( $m$  and  $n$ ) are removed. The final modified circuit is shown in Fig. 4(b), where the transformation reduces the number of stressed PMOS transistors and hence mitigates NBTI-induced degradation.

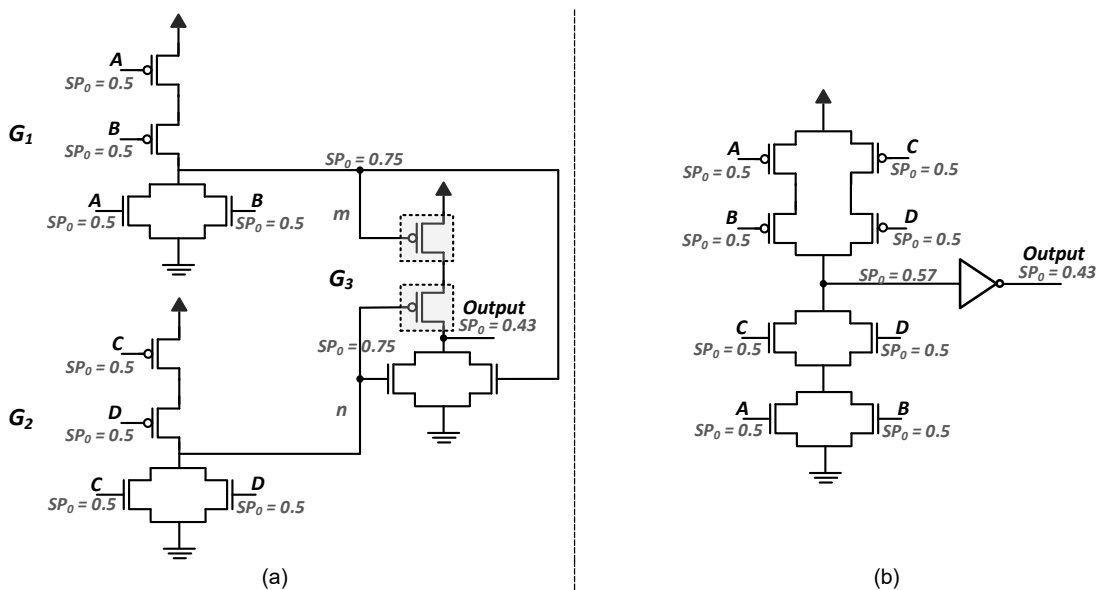


Fig. 4. An example of converting sensitizer and sensitive gates into a complex gate and removing internal NBTI-critical nodes; a) 3-input NOR circuit, and b) its equivalent NBTI-tolerant circuit.

A second example is presented in Fig. 5(a), which depicts a gate-level combinational circuit. Based on the  $SP_0$  values shown, and assuming an optimal threshold value of 0.75, internal nodes  $N_7$  and  $N_8$  are identified as NBTI-critical nodes. Accordingly, gates  $G_1$  and  $G_2$  are classified as sensitizer gates, while gates  $G_3$ ,  $G_4$ , and  $G_5$  are identified as sensitive gates. The PMOS transistors in  $G_3$ ,  $G_4$ , and  $G_5$  are therefore subject to significant NBTI stress. In this circuit, the critical path is  $G_0 \rightarrow G_2 \rightarrow G_4 \rightarrow G_7 \rightarrow G_8$ . According to Algorithm 3, because sensitizer

gates  $G_1$  and  $G_2$  each have two fan-out branches, duplicate versions of these gates ( $G_1'$  and  $G_2'$ ) are instantiated to enable individual merging with their respective sensitive gates (as shown in Fig. 5(b)).

In the critical path, gates  $G_1'$  and  $G_2$  are merged with sensitive gate  $G_4$  to form complex gate  $U_1$ , while  $G_2'$  and  $G_5$  are merged into complex gate  $U_2$ . These complex gates are then inserted into the circuit, replacing the original ones. Subsequently, in the non-critical paths, gates  $G_1$  and  $G_3$  are merged to form complex gate  $U_0$ , which also replaces the original components. Through this transformation process, all identified NBTI-critical internal nodes and their associated PMOS transistors are effectively eliminated. As a result, the overall NBTI stress within the circuit is reduced, and the method successfully mitigates NBTI-induced degradation.

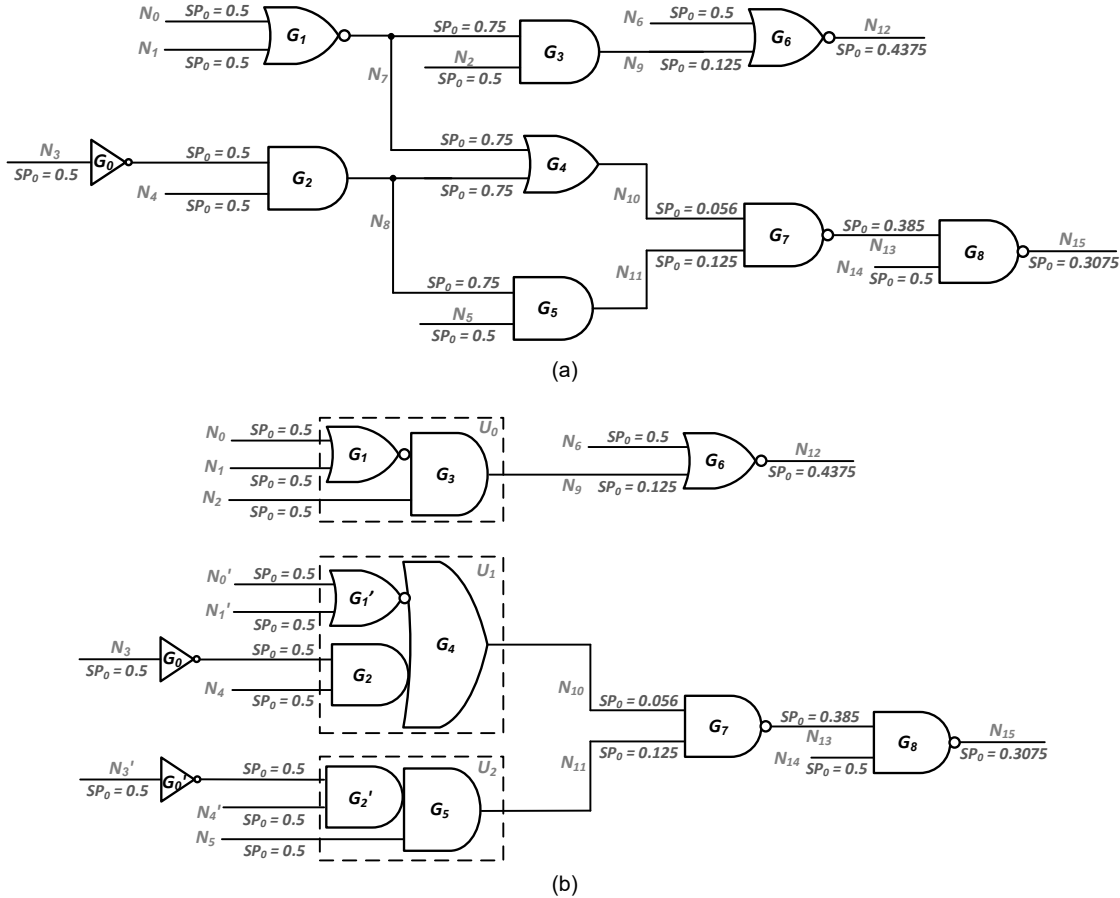


Fig. 5. An example of applying the proposed gate merging method to a combinational circuit;  $SP_0$  values of the circuit node: a) before gate merging, and b) after gate merging.

## 5- Simulation Result

The effectiveness of the proposed method has been evaluated on a subset of combinational and sequential circuits from the ISCAS'85 and ISCAS'89 benchmark suites. The algorithms were implemented in the C programming language. Each benchmark circuit was simulated using 10,000 random input vectors. Transistor-level simulations incorporating NBTI modeling were conducted using the MOS reliability analysis (MOSRA) model in Synopsys HSPICE, based on the 45nm planar predictive technology model (PTM) [37, 38]. The supply voltage was set to 1V, and all circuits were subjected to NBTI stress for 10 years. Area comparisons were calculated based on the sum of transistor widths, which is an accepted metric for planar CMOS technologies [39].

The proposed gate merging method removes NBTI-critical internal nodes, thereby eliminating transistors with high  $SP_0$  values from the modified circuits. However, to ensure an effective reduction in NBTI-induced delay degradation, it is necessary to first determine the optimal  $SP_0$  threshold value for each circuit. Fig. 6 illustrates the normalized PPC for various threshold values applied to the S298 circuit. The PPC values have been normalized with respect to the PPC of the unmodified (base) circuit.

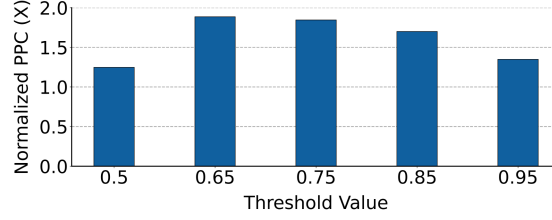


Fig. 6. Normalized PPC to base circuit for various threshold values in the gate merging method applied to the S298 circuit.

In this example, the threshold value 0.65 yields the maximum PPC and is therefore selected as the optimal threshold. It is notable that for all tested thresholds, the PPC of the modified circuit exceeds that of the base circuit, indicating that the delay reduction outweighs the area overhead introduced by gate merging.

Additionally, Fig. 7 presents the  $SP_0$  distribution of PMOS transistors in the S208 circuit, both before and after the application of the proposed method. The horizontal axis represents  $SP_0$  values, while the vertical axis shows the number of nodes corresponding to each  $SP_0$ . The results demonstrate a significant reduction in the number of high- $SP_0$  nodes after applying the method, effectively mitigating NBTI-induced degradation. Notably, no nodes with  $SP_0 > 0.8$  remain in the modified circuit. It is worth noting that the number of PMOS transistors differs before and after applying the proposed method.

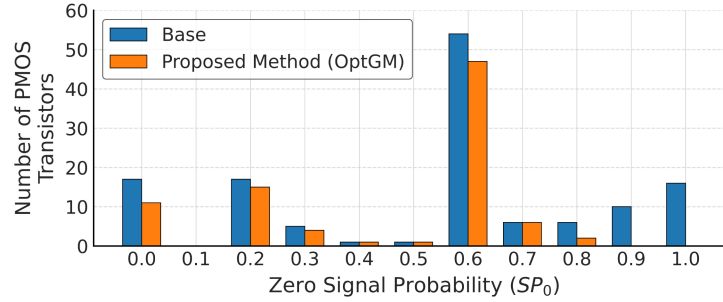


Fig. 7.  $SP_0$  distribution of PMOS transistors in the S208 circuit before and after applying the proposed method.

Table 2 reports the critical path delays of various benchmark circuits before and after NBTI stress, both for the base circuits and for those improved using OptGM. The second and fourth columns show delays before stress, while the third and sixth columns show delays after 10 years of NBTI aging. The optimal  $SP_0$  threshold value used for each circuit is listed in the fifth column. Columns seven and eight indicate the percentage of delay improvement achieved by the OptGM method before and after NBTI stress, respectively. On average, the proposed method improves pre-stress delay by 8.39%, and post-stress delay by 23.87%. Statistical analysis with 95% confidence indicates that OptGM achieves an NBTI-induced delay degradation improvement within the range of 16.73% to 31.01% for similar circuits using the same technology model.

Table 2. Delay results for the base and OptGM-enhanced circuits before and after NBTI stress

Circuit	Base circuit		Proposed method (OptGM)			OptGM method improvement	
	Delay (ps) before stress	Delay (ps) after stress	Delay (ps) before stress	Optimal threshold value	Delay (ps) after stress	Delay (%) before stress	Delay (%) after stress
S27	20.2	40.5	20.3	0.75	38.6	-0.50	4.69
S208	176.0	287	166	0.75	247	5.68	13.94
S298	263.0	449	260	0.65	352	1.14	21.60
S400	15.9	27.2	15.8	0.65	20.2	0.63	25.73
C432	189.2	352.2	159.6	0.5	203	15.64	42.36
C1355	169.0	284.0	161.0	0.65	229.5	4.73	19.21
C2670	227.5	402.0	208.1	0.85	320.1	8.49	20.37
C1908	229.8	392.3	210.8	0.85	320.7	8.24	18.25
C3540	290.2	487.7	252.7	0.75	327.6	12.93	32.81
C5315	221.2	391.0	185.8	0.65	285.7	16.02	26.94
C6288	928.7	1514.4	749.5	0.5	959.8	19.29	36.62
<b>Average</b>						<b>8.39</b>	<b>23.87</b>

Table 3 presents the transistor count, number of NBTI-critical PMOS transistors, and area overhead before and after applying OptGM. On average, OptGM eliminates 89.29% of NBTI-critical transistors (i.e., PMOS transistors connected to critical nodes). It is worth mentioning that, while the proposed method primarily targets the elimination of PMOS transistors that are frequently on, the merging of gates also results in the removal of associated NMOS transistors, which are typically in the off state. Consequently, the likelihood of increased NMOS stress—and thus PBTI degradation—is minimal, or may even be slightly reduced. Furthermore, most circuits utilize fewer total transistors after modification, due to the consolidation of logic into complex gates. However, in cases where sensitizer gates have multiple fan-out branches, duplication of gates is required for each sensitive gate, potentially increasing the area, which results in an average 1.8% increased area. For example, in the S27 circuit, two sensitizer gates with dual fan-outs lead to duplication, increasing the area. Conversely, in many other circuits, the area reduction from gate merging exceeds the overhead from duplication.

Table 3. Area results of base circuits and those modified with OptGM

Circuit	Base circuit			Proposed method (OptGM)			OptGM method improvement		Area overhead (%)
	Total transistors (#)	Critical transistors (#)	Sum of transistors' width (mm)	Total transistors (#)	Critical transistors (#)	Sum of transistors' width (mm)	Reduction of total transistors (%)	Reduction of critical transistors (%)	
S27	42	3	3.98	48	0	5.60	-14.3	100.0	40.7
S208	478	32	64.9	448	2	62.28	6.3	93.8	-4.0
S298	782	66	39.54	693	8	37.83	11.4	87.9	-4.3
S400	850	26	95.28	795	0	76.89	6.5	100.0	1.3
C432	832	76	139.58	736	5	98.8	11.5	93.4	-19.2
C1355	2356	104	201.28	2116	10	212.53	10.1	90.4	5.6
C2670	1526	218	789.12	1366	54	729.34	10.5	75.2	7.57
C1908	5082	199	495.49	4584	32	486.3	9.8	83.91	1.86
C3540	2167	532	1153.93	1977	88	1116.43	8.77	83.45	3.35
C5315	3025	754	1670.94	3014	105	2005.13	0.36	86.07	-0.2
C6288	2672	890	1591.2	2396	96	1788.50	10.32	89.21	-12.4
<b>Average</b>							<b>6.47</b>	<b>89.29</b>	<b>1.8</b>

Table 4 reports the average  $SP_0$  values before and after applying OptGM. The method achieves a mean reduction in  $SP_0$  of 28.76%, effectively reducing the NBTI stress time of transistors. Since NBTI-induced threshold voltage shifts are strongly time-dependent, reducing stress duration leads to substantial reliability improvement.

Table 4. Average  $SP_0$  of benchmark circuits before and after applying the proposed method

Circuit	Average $SP_0$ of base circuit	Average $SP_0$ of modified circuit	Average $SP_0$ reduction (%)
S27	0.56	0.53	5.36
S208	0.47	0.34	27.66
S298	0.53	0.38	28.30
S400	0.49	0.28	42.86
C432	0.48	0.30	37.50
C1355	0.46	0.32	35.43
C2670	0.41	0.34	15.93
C1908	0.58	0.46	20.16
C3540	0.69	0.39	33.47
C5315	0.45	0.34	28.88
C6288	0.49	0.29	40.82
<b>Average</b>			<b>28.76</b>

Fig. 8 shows the percentage of NBTI-induced delay degradation reduction for different durations of NBTI stress—5, 10, 30, and 50 years—under a fixed threshold value of 0.75. The base and modified circuits have been simulated for different years under NBTI stress, and the percentage of delay improvement has been reported. The results show the improvement percentage increases when the stress time increases. Therefore, the proposed method increases performance in longer stress time efficiently.

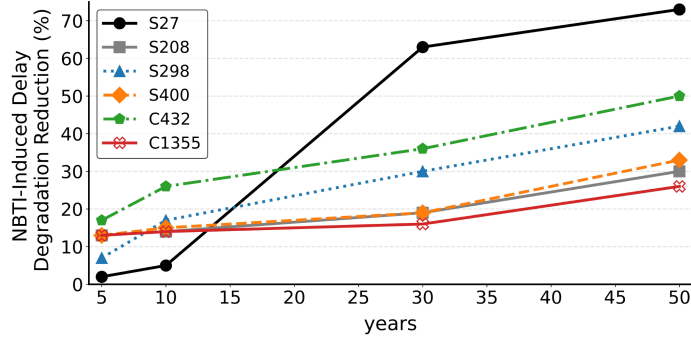
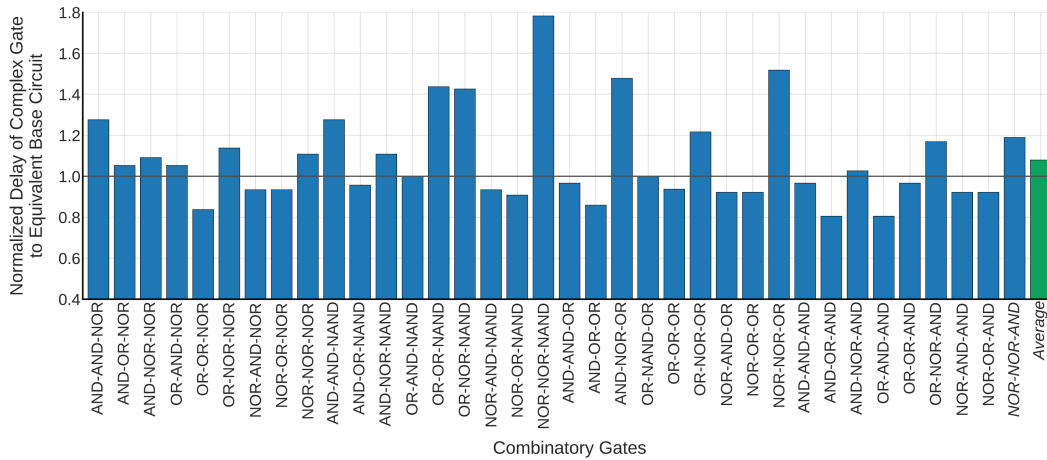
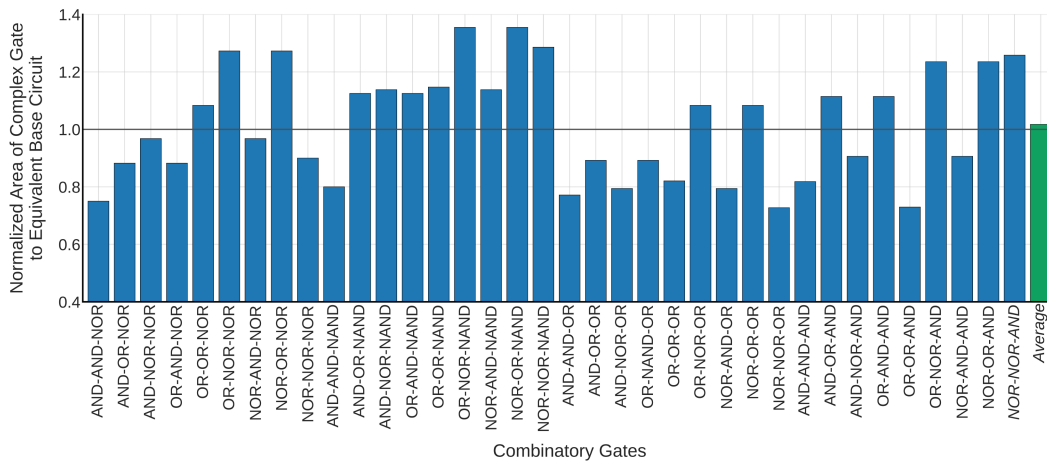


Fig. 8. The percentage of NBTI-induced delay degradation reduction under 5, 10, 30, and 50 years NBTI stress on benchmark circuits (OptGM modified vs. base circuit).

Fig. 9(a) and Fig. 9(b) present a comparison of delay and area, respectively, for original circuits and their equivalent complex gates. The vertical axis shows the ratio of the complex gate metric to the equivalent metric in its base circuit. Based on the results, the average delay of complex gates is approximately 7% higher than that of their equivalent primary-gate implementations. However, Fig. 9(b) shows that the average complex gate area is nearly equal to that of its equivalent circuit. Note that when  $n$  fan-outs exist for a sensitizer gate,  $n$  identical copies are generated—contributing to area growth in some cases.



(a)



(b)

Fig. 9. Comparison of original circuits and their equivalent complex gates in terms of a) delay and, b) area.

Table 5 compares the PPC values for gate merging with fixed and variable threshold values. Method [14] used a fixed threshold of 0.75, while the proposed method (OptGM) operates under variable threshold values and determines an optimal threshold for each circuit. On average, the proposed method improves PPC by 12.8% over the method [14]. Furthermore, in comparison with other related studies, OptGM reduces NBTI-induced degradation by 23.87% and removes 89.29% of NBTI-critical transistors, whereas prior methods [15] and [40] reported improvements of 32.36% and 1.21%, respectively.

Table 5. Comparison of PPC for gate merging methods with fixed and variable threshold values

Circuit	PPC value of method [14]	Threshold value of OptGM method	PPC of OptGM method	PPC improvement (%)
S27	1.77	0.75	1.77	0.00
S280	1.12	0.75	1.12	0.00
S298	1.21	0.65	1.22	0.81
S400	1.00	0.65	1.36	36.25
C432	1.11	0.50	1.46	31.17
C1355	1.20	0.65	1.31	8.93
<b>Average</b>				<b>12.80</b>

## 6- Conclusion

As technology scales down, NBTI has become a major reliability concern in modern CMOS circuits due to its impact on PMOS threshold voltage and circuit delay. This paper proposed OptGM, an optimized gate merging method that effectively mitigates NBTI-induced degradation by eliminating NBTI-critical internal nodes through SP0-based analysis and logic gate merging. Unlike prior methods, OptGM adaptively selects the optimal threshold per circuit using a performance-per-cost metric, enabling a better trade-off between NBTI mitigation and overhead. Simulation results on standard benchmarks demonstrated that OptGM reduces NBTI-induced delay degradation by 23.87%, removes 89.29% of NBTI-critical transistors, and improves PPC by 12.8%, with minimal area overhead—highlighting its effectiveness. As future work, the development of advanced optimization metrics incorporating multiple design parameters with tunable priorities, along with the integration into logic synthesis tools, can be explored to support fully automated NBTI-aware ASIC design flows.

## References

- [1] X. Yang, Q. Sang, C. Wang, M. Yu, and Y. Zhao, "Development and Challenges of Reliability Modeling from Transistors to Circuits," *IEEE Journal of the Electron Devices Society*, vol. 11, pp. 179–189, 2023.
- [2] K. Singh and J. Mahur, "Deep Insights of Negative Bias Temperature Instability (NBTI) Degradation," *IEEE International Students' Conference on Electrical, Electronics and Computer Science*, pp. 1-5, 2025.
- [3] K. Singh, S. Kalra, and J. Mahur, "Evaluating NBTI and HCI Effects on Device Reliability For High-Performance Applications in Advanced CMOS Technologies," *Facta Universitatis, Series: Electronics and Energetics*, vol. 37, no. 4, pp. 581–597, 2024.
- [4] Z. Sun, S. Chen, L. Zhang, R. Huang, and R. Wang, "The Understanding and Compact Modeling of Reliability in Modern Metal–Oxide–Semiconductor Field-Effect Transistors: From Single-Mode to Mixed-Mode Mechanisms," *Micromachines*, vol. 15, no. 1, p. 127, 2024.
- [5] Y. Xue *et al.*, "Investigation of Positive Bias Temperature Instability in advanced FinFET nodes," *IEEE International Reliability Physics Symposium Proceedings*, pp. 1-5, 2024.
- [6] Y. Wang, Y. Li, Y. Yang, and W. Chen, "Hot Carrier Injection Reliability in Nanoscale Field Effect Transistors: Modeling and Simulation Methods," *Electronics*, vol. 11, no. 21, p. 3601, 2022.
- [7] W. S. Zhao, R. Zhang, and D. W. Wang, "Recent Progress in Physics-based Modeling of Electromigration in Integrated Circuit Interconnects," *Micromachines*, vol. 113, no. 6, p. 883, 2022.
- [8] L. Lanzieri, G. Martino, G. Fey, H. Schlarb, T. C. Schmidt, and M. Wählisch, "A Review of Techniques for Ageing Detection and Monitoring on Embedded Systems," *ACM Computing Surveys*, vol. 57, no. 24, pp. 1-34, 2024.
- [9] M. Wang, "A Review of Reliability in Gate-All-Around Nanosheet Devices," *Micromachines*, vol. 15, no. 2, p. 269, 2024.
- [10] S. Mahapatra, "Recent Advances in PMOS Negative Bias Temperature Instability: Characterization and Modeling of Device Architecture, Material and Process Impact," *Recent Advances in PMOS Negative Bias Temperature Instability: Characterization and Modeling of Device Architecture, Material and Process Impact*, pp. 1–311, 2021.
- [11] A. Bhattacharjee, A. Das, D. K. Sahu, S. N. Pradhan, and K. Das, "A Meta-Heuristic Search-Based Input Vector Control

- Approach to Co-Optimize NBTI Effect, PBTI Effect, and Leakage Power Simultaneously," *Microelectronics Reliability*, vol. 144, p. 114979, 2023.
- [12] A. Thirunavukkarasu *et al.*, "Device to Circuit Framework for Activity-Dependent NBTI Aging in Digital Circuits," *IEEE Trans Electron Devices*, vol. 66, no. 1, pp. 316–323, 2019.
- [13] S. Kiamehr, F. Firouzi, and M. B. Tahoori, "Input and Transistor Reordering for NBTI and HCI Reduction in Complex CMOS Gates," *Proceedings of the ACM Great Lakes Symposium on VLSI (GLSVLSI)*, pp. 201–206, 2012.
- [14] M. Ghane and H. R. Zarandi, "Gate Merging: An NBTI Mitigation Method to Eliminate Critical Internal Nodes in Digital Circuits," *24th Euromicro International Conference on Parallel, Distributed, and Network-Based Processing (PDP)*, pp. 786–791, 2016.
- [15] I. C. Lin, C. H. Lin, and K. H. Li, "Leakage and Aging Optimization Using Transmission Gate-Based Technique," *IEEE Transactions on Computer-Aided Design of Integrated Circuits and Systems*, vol. 32, no. 1, pp. 87–99, 2013.
- [16] Y. G. Chen, H. Y. Yang, and I. C. Lin, "GNN-Based INC and IVC Co-Optimization for Aging Mitigation," *European Test Symposium (ETS)*, pp. 1-4, 2024.
- [17] Y. Wang, X. Chen, W. Wang, Y. Cao, Y. Xie, and H. Yang, "Leakage Power and Circuit Aging Co-optimization By Gate Replacement Techniques," *IEEE Trans Very Large Scale Integr VLSI Syst*, vol. 19, no. 4, pp. 615–628, 2011.
- [18] A. Bhattacharjee, A. Nag, K. Das, and S. N. Pradhan, "Design of Power Gated SRAM Cell for Reducing the NBTI Effect and Leakage Power Dissipation During the Hold Operation," *Journal of Electronic Testing: Theory and Applications (JETTA)*, vol. 38, no. 1, pp. 91–105, 2022.
- [19] J. F. Zhang, R. Gao, M. Duan, Z. Ji, W. Zhang, and J. Marsland, "Bias Temperature Instability of MOSFETs: Physical Processes, Models, and Prediction," *Electronics*, vol. 11, no. 9, p. 1420, 2022.
- [20] W. Chen, L. Xiong, M. Zheng, S. He, and L. Cai, "Open Model Interface Assisted NBTI-Aware Design with Dual-Vth Logic Synthesis Strategy for Reliability Improvement," *IEEE Transactions on Device and Materials Reliability*, 2025.
- [21] Z. Amini-sheshdeh and A. Nabavi, "Design of Improved-Reliability Nanocircuits with Mixed NBTI- and HCI-Aware Gate-Sizing Formulation," *IEEE Transactions on Electrical and Electronic Engineering*, vol. 8, no. 6, pp. 587–590, 2013.
- [22] L. Xiong, W. Chen, M. Zheng, and L. Cai, "Gate Sizing and Buffer Insertion for Circuit Aging and Thermal Resilience Enhancement," *Microelectronics Reliability*, vol. 166, p. 115604, 2025.
- [23] J. H. Han *et al.*, "Tuning the Threshold Voltage of an Oxide Thin-Film Transistor by Electron Injection Control Using a p–n Semiconductor Heterojunction Structure," *Applied Materials and Interfaces*, vol. 16, no. 24, pp. 31254–31260, 2024.
- [24] Kajal and V. K. Sharma, "NBTI Effect Survey for Low Power Systems in Ultra-Nanoregime," *Current Nanoscience*, vol. 20, no. 3, pp. 298–313, 2023.
- [25] A. Gomez and V. Champac, "An Efficient Metric-Guided Gate Sizing Methodology for Guardband Reduction Under Process Variations and Aging Effects," *Journal of Electronic Testing: Theory and Applications (JETTA)*, vol. 35, no. 1, pp. 87–100, 2019.
- [26] H. Xu *et al.*, "Novel Critical Gate-Based Circuit Path-Level NBTI-Aware Aging Circuit Degradation Prediction," *Journal of Circuits, Systems and Computers*, vol. 32, no. 10, p. 2350175, 2023.
- [27] K. Singh and S. Kalra, "A Comprehensive Assessment of Current Trends in Negative Bias Temperature Instability (NBTI) Deterioration," *International Conference on Signal Processing and Communication (ICSC)*, pp. 271–276, 2021.
- [28] S. Seckiner, L. Wang, and S. Kose, "An NBTI-Aware Digital Low-Dropout Regulator with Adaptive Gain Scaling Control," *IEEE/IFIP International Conference on VLSI and System-on-Chip (VLSI-SoC)*, pp. 191–196, 2019.
- [29] D. R. Bild, G. E. Bok, and R. P. Dick, "Minimization of NBTI Performance Degradation Using Internal Node Control," *Proceedings -Design, Automation and Test in Europe (DATE)*, pp. 148–153, 2009.
- [30] H. Mostafa, M. Anis, and M. Elmasry, "NBTI and Process Variations Compensation Circuits Using Adaptive Body Bias," *IEEE Transactions on Semiconductor Manufacturing*, vol. 25, no. 3, pp. 460–467, 2012.
- [31] Y. Lee and T. Kim, "A Fine-Grained Technique of NBTI-Aware Voltage Scaling and Body Biasing for Standard Cell Based Designs," *Proceedings of the Asia and South Pacific Design Automation Conference (ASP-DAC)*, pp. 603–608, 2011.
- [32] A. P. Shah, N. Yadav, A. Beohar, and S. K. Vishvakarma, "On-chip Adaptive Body Bias for Reducing The Impact of NBTI on 6T SRAM Cells," *IEEE Transactions on Semiconductor Manufacturing*, vol. 31, no. 2, pp. 242–249, 2018.
- [33] M. Basoglu, M. Orshansky, and M. Erez, "NBTI-Aware DVFS: A New Approach to Saving Energy and Increasing Processor Lifetime," *Proceedings of the International Symposium on Low Power Electronics and Design*, pp. 253–258, 2010.
- [34] S. V. Kumar, C. H. Kim, and S. S. Sapatnekar, "Adaptive Techniques for Overcoming Performance Degradation due to Aging in Digital Circuits," *Proceedings of the Asia and South Pacific Design Automation Conference (ASP-DAC)*, pp. 284–289, 2009.
- [35] N. H.E.Weste and D. M. Harris, "CMOS Technologies," *CMOS VLSI Design: A Circuits and Systems Perspective*, 2015.
- [36] N. Kito, T. Kawaguchi, K. Takagi, and N. Takagi, "Technology Mapping With Clockless Gates for Logic Stage Reduction of RSFQ Logic Circuits," *IEEE Transactions on Applied Superconductivity*, vol. 33, no. 5, 2023.
- [37] B. Tudor *et al.*, "MOSRA: An Efficient and Versatile MOS Aging Modeling and Reliability Analysis Solution for 45nm

- and Below," *IEEE International Conference on Solid-State and Integrated Circuit Technology*, pp. 1645–1647, 2010.
- [38] A. Bu, R. Wang, S. Jia, and J. Li, "GPR-Based Framework for Statistical Analysis of Gate Delay under NBTI and Process Variation Effects," *Electronics*, vol. 11, no. 9, 2022.
- [39] S. M. Sze, Yiming. Li, and K. Kwok. Ng, "Physics of Semiconductor Devices," John wiley & sons, p. 931, 2021.
- [40] K. C. Wu and D. Marculescu, "Aging-Aware Timing Analysis and Optimization Considering Path Sensitization," *Design, Automation and Test in Europe (DATE)*, pp. 1572–1577, 2011.